

Geophysics and Site Characterization at the Hanford Site: The Successful Use of Electrical Resistivity to Position Boreholes to Define Deep Vadose Zone Contamination-11509

Malcolm J. Gander,* Kevin D. Leary,** Marc T. Levitt,***

Charles W. Miller,* Dale F. Rucker***

*CH2M HILL Plateau Remediation Company

**U.S. Department of Energy, Richland Operations Office

***hydroGEOPHYSICS, Inc.

ABSTRACT

Historic boreholes confirmed the presence of nitrate and radionuclide contaminants at various intervals throughout a more than 60 m (200 ft) thick vadose zone, and a 2010 electrical resistivity survey mapped the known contamination and indicated areas of similar contaminants, both laterally and at depth; therefore, electrical resistivity mapping can be used to more accurately locate characterization boreholes.

At the Hanford Nuclear Reservation in eastern Washington, production of uranium and plutonium resulted in the planned release of large quantities of contaminated wastewater to unlined excavations (cribs). From 1952 until 1960, the 216-U-8 Crib received approximately 379,000,000 L (100,000,000 gal) of wastewater containing 25,500 kg (56,218 lb) uranium; 1,029,000 kg (1,013 tons) of nitrate; 2.7 Ci of technetium-99; and other fission products including strontium-90 and cesium-137. The 216-U-8 Crib reportedly holds the largest inventory of waste uranium of any crib on the Hanford Site.

Electrical resistivity is a geophysical technique capable of identifying contrasting physical properties; specifically, electrically conductive material, relative to resistive native soil, can be mapped in the subsurface. At the 216-U-8 Crib, high nitrate concentrations (from the release of nitric acid [HNO₃] and associated uranium and other fission products) were detected in 1994 and 2004 boreholes at various depths, such as at the base of the Crib at 9 m (30 ft) below ground surface (bgs) and sporadically to depths in excess of 60 m (200 ft) bgs. These contaminant concentrations were directly correlative with the presence of observed low electrical resistivity responses delineated during the summer 2010 geophysical survey.

Based on this correlation and the recently completed mapping of the electrically conductive material, additional boreholes are planned for early 2011 to identify nitrate and radionuclide contamination: a) throughout the entire vertical length of the vadose zone (i.e., 79 m [260 ft] bgs) within the footprint of the Crib, and b) 15 to 30 m (50 to 100 ft) east of the Crib footprint, where contaminants are inferred to have migrated through relatively permeable soils.

Confirmation of the presence of contamination in historic boreholes correlates well with mapping from the 2010 survey, and serves as a basis to site future characterization boreholes that will likely intersect contamination both laterally and at depth.

INTRODUCTION

A non-invasive electrical resistivity geophysical survey was conducted the summer of 2010 over two waste disposal excavations, or cribs (the 216-U-8 Crib and 216-U-12 Crib), adjacent to the U-Plant within the 200-West Area of the Hanford Nuclear Reservation (Hanford Site) in eastern Washington (Fig. 1). The purpose of the survey was to collect information from the subsurface to identify soils that are electrically conductive (relative to resistive native soil) from contaminated wastewater resulting from the

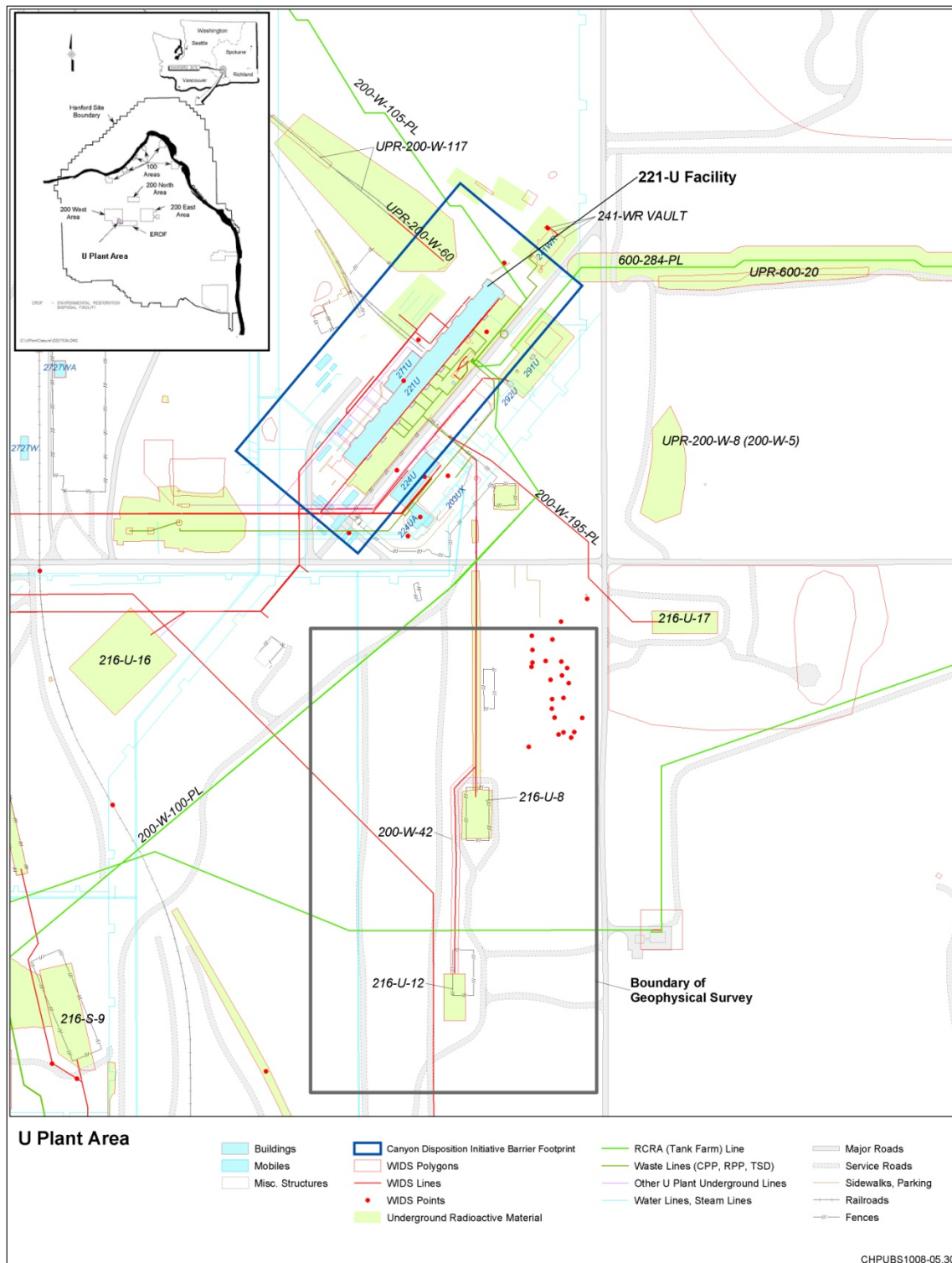


Fig. 1. U-Plant Complex showing the boundary of the geophysical survey and inset of the site location.

chemical separation of uranium. Previous characterization boreholes verified the presence of uranium, technetium-99, and nitrate contamination within and beneath the 216-U-8 Crib (U-8 Crib) and the 216-U-12 Crib (U-12 Crib) in areas of electrically conductive soils, as shown by the 2010 geophysical survey; therefore, the geophysical survey results could be used with a high degree of confidence to guide the placement of additional characterization boreholes in the vicinity of the U-8 and U-12 Crib. Specifically, the completion of additional boreholes is to support the following:

- Characterization of the deep vadose zone contamination
- Evaluation of current and future groundwater protection concerns
- Evaluation of remedial alternatives
- Final remedial decision making.

The Hanford Site is a 1,517 km² (586 mi²) federal facility located along the Columbia River. From 1943 to 1990, the primary mission of the Hanford Site was the production of nuclear materials for national defense. In July 1989, the Hanford Site was placed on the National Priorities List [1] pursuant to the *Comprehensive Environmental Response, Compensation, and Liability Act of 1980 (CERCLA)* [2].

Portions of the Hanford Site are on the U.S. Environmental Protection Agency's (EPA) CERCLA National Priorities List. The work for cleanup of these National Priorities List sites is in accordance with the National Contingency Plan regulations [1] and, where applicable, the *Hanford Federal Facility Agreement and Consent Order (Tri-Party Agreement)* [3].

BACKGROUND

Fig. 1 presents a detailed layout of the U-Plant complex, its connection to the U-8 and U-12 Crib, and the boundary of the 37-acre area addressed in the geophysical survey.

The U-8 Crib is an inactive wastewater disposal site consisting of a series of three wooden cribbed timber structures in an unlined excavation approximately 9 m (30 ft) deep (Fig. 2). The U-8 Crib was designed to provide a means to discharge contaminated wastewater directly to the soil column. Previous characterization work indicates that the U-8 Crib vadose zone is known to contain subsurface soil contamination by radioactive and nonradioactive plant-related contaminants. The volume of wastewater discharged to the Crib was sufficient enough to cause the water and some of the dissolved waste constituents to reach the underlying groundwater. A total of 379,000,000 L (approximately 100,000,000 gal) of radiologically contaminated wastewater (mostly process condensate) was discharged to this Crib from June 1952 to March 1960. The discharges contained an estimated 25,500 kg (55,125 lb, or approximately 28 tons) of uranium; 1,029,000 kg (1,134 tons) of nitrate; 2.7 Ci of technetium-99; and other fission products (e.g., strontium-90 and cesium-137). Estimated releases were calculated using the *Hanford Soil Inventory Model* [4].

The majority of previous characterization efforts have focused on quantifying relatively shallow soil contamination to identify the extent of lateral spreading of contamination and estimate the size of a cap for a surface remedy. Only one borehole, drilled in 1994, extended deeper than about 15 m (50 ft) below ground surface (bgs). This single deep borehole, identified as 299-W19-94, was located within the excavation footprint of the Crib (Fig. 2). This borehole was advanced to a total depth of approximately 61 m (200 ft) bgs. Soil samples were collected from selected depth intervals and subsequently analyzed for specific contaminants. The sampling and analysis results indicated the presence of facility-related radioactive and nonradioactive contaminants at varying concentrations throughout that portion of the vadose zone that was examined. The deepest sample collection did not extend below the fine-textured soil

formation known as the Cold Creek unit, located within the lower third of the vadose zone at most locations in the 200-West Area. As a result of this limited extent of vertical soil examination, no

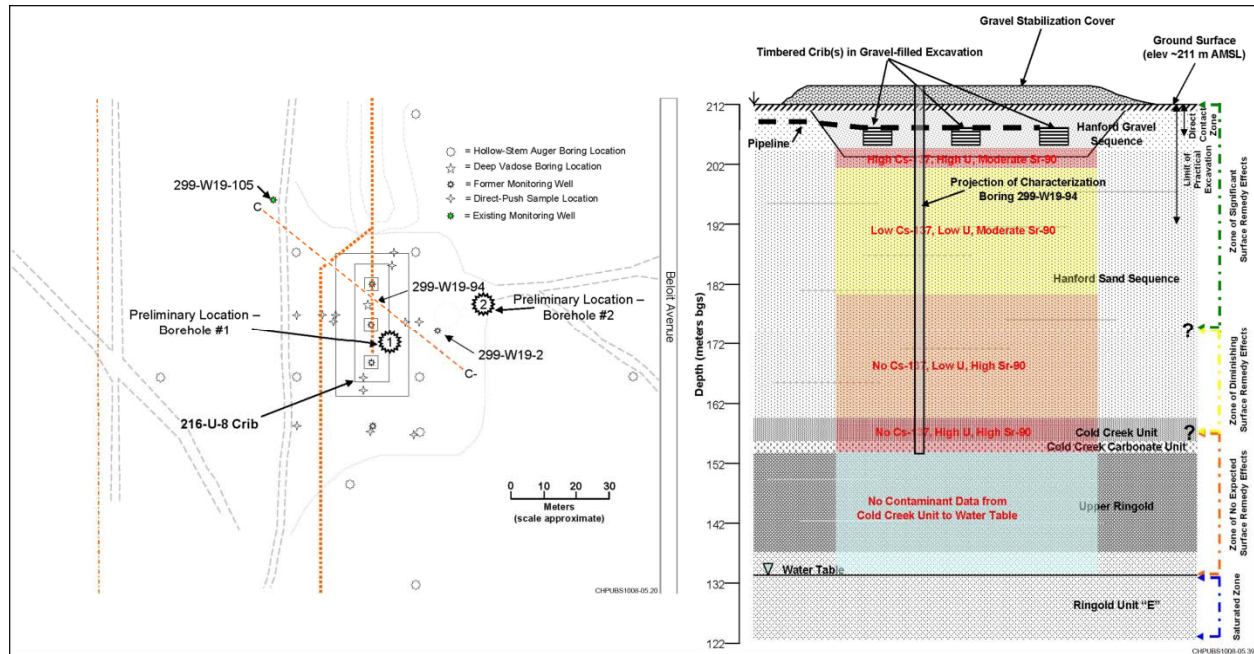


Fig. 2a. 216-U-8 Crib proposed borehole locations, showing select historic boreholes (on left). Fig. 2b. 216-U-8 Crib showing contaminant distribution and extent of vertical characterization.

observations or measurements are available to describe residual contamination within the vadose zone beneath the Cold Creek unit and above the current groundwater table.

The U-12 Crib is an inactive wastewater disposal site located south of the U-12 Crib (Fig. 1). The site consists of a perforated 30 cm (12 in.) diameter vitrified clay pipe placed in an unlined, gravel-filled excavation approximately 5 m (15 ft) deep (Fig. 3). The U-12 Crib was designed to provide a means to discharge contaminated wastewater directly to the soil column. The waste stream discharged to the 216-U-12 Crib consisted primarily of acidic, radiologically contaminated condensate generated by the calcining and nitric acid recovery processes associated with the uranium oxide (UO₃) process performed in the 224-U Building. Based on historical information and previous soil characterization and groundwater monitoring, the 216-U-12 Crib vadose zone is known to contain subsurface soil contamination by radioactive and nonradioactive plant-related contaminants.

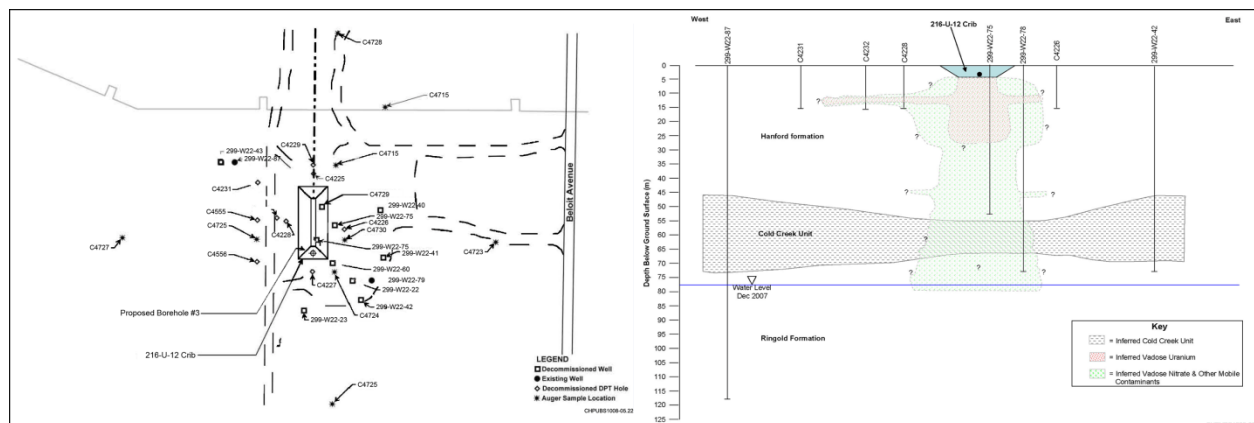


Fig. 3a. 216-U-12 showing the proposed borehole location and historic boreholes (above). Fig. 3b. Conceptual contaminant distribution for the 216-U-12 Crib.

The volume of wastewater historically discharged to the Crib was sufficient to cause the water and some of the dissolved waste constituents to reach the underlying groundwater. A total of approximately 150 million L (approximately 39.6 million gal) of acidic wastewater was discharged to the crib from 1960 to 1988. The discharges contained an estimated 6,458 kg (6.36 tons) of uranium; 2.3 million kg (2,264 tons) of nitrate; 1 Ci of technetium-99; and other fission products (e.g., tritium, strontium-90, and cesium-137). Estimated releases were calculated using the *Hanford Soil Inventory Model* [4].

The majority of previous characterization efforts have focused on quantifying relatively shallow soil contamination to identify the extent of lateral spreading of contamination and estimate the size of a cap for a surface remedy. Only one borehole, identified as 299-W22-78, drilled in 1994, extended deeper than about 50 m (164 ft) bgs (Fig. 3). This single deep borehole was located outside the Crib excavation footprint, immediately to the east of the Crib. This borehole was advanced to a total depth of approximately 70.9 m (233 ft) bgs, where the water table was encountered. A total of 17 soil samples were collected from selected depth intervals and subsequently analyzed for specific contaminants. Results of sampling and analysis indicated the discontinuous presence of facility-related radioactive and nonradioactive contaminants at varying concentrations throughout the portion of the vadose zone that was examined.

The deepest sample collection extended below the fine-textured soil formation known as the Cold Creek unit, located within the lower third of the vadose zone at most locations in the 200-West Area.

Although the characterization borehole at the U-12 Crib did extend from the ground surface to the water table of the underlying unconfined aquifer, the discontinuous distribution of site-related contaminants suggests that this boring location may not have penetrated the most highly contaminated portion of the vadose zone beneath the Crib. In addition, the historical discharge of strongly acidic wastewater to the crib may have affected the contaminant transport characteristics of the vadose zone at this site. Analysis of soil samples for some fission products associated with the waste stream (e.g., cesium-137 and strontium-90) as well as nonradioactive metals was only performed on one soil sample collected from a shallow (and apparently unaffected), near-surface depth interval. Only one sample was analyzed for organic constituents (i.e., volatile compounds and kerosene-range petroleum hydrocarbons); none were detected.

GEOLOGY AND HYDROGEOLOGY

The geology of the subsurface in the vicinity of the U-8 and U-12 Cribs consists of a basal basalt bedrock unit, assigned to the Tertiary Columbia River Basalt Group. Unconsolidated sediments of the Miocene-Pliocene Ringold Formation overlie the bedrock, which in turn are overlain by the Cold Creek unit and the Pleistocene Hanford formation, which occurs beneath a thin 3-5 m (10-15 ft) veneer of surficial recent eolian and alluvial deposits [5]. The Ringold Formation is interpreted as consisting of continental fluvial and lacustrine sediments deposited by the ancestral Columbia and Clearwater-Salmon Rivers [6]. The Hanford formation is interpreted as consisting of cataclysmic flood deposits in the Pasco Basin [7].

Geologic logs of boreholes beneath and immediately adjacent to the U-8 and U-12 Cribs indicate that the unconsolidated sediments of the Hanford formation and the Ringold Formation are predominantly sand with subordinate amounts of silt. The fine-grained and carbonate-rich Cold Creek unit is a relatively thin but significant depositional unit that represents post-Ringold and pre-Hanford sedimentation. The Cold Creek unit occurs between approximately 52-57 m (170-185 ft) beneath the U-8 Crib, based on the geologic log of borehole 299-W19-94 (Fig. 2b). Beneath the U-12 Crib, the Cold Creek unit is

approximately 14 m (45 ft) thick, based on the geologic log of borehole 299-WW22-78 (Fig. 3b) [8]. Historic exploration and laboratory analysis of contaminants from the Cold Creek unit indicate that this unit may preferentially concentrate contaminants by virtue of its fine-grained and calcium carbonate-bearing characteristics.

Groundwater beneath the U-8 and U-12 Cribs is currently approximately at 79 m bgs (260 ft), based on July 2010 depth-to-water information measured in well 299-W19-105. This uppermost water-bearing zone is unconfined [9]. The groundwater flow direction as calculated from wells in the immediate vicinity is toward the southeast. Within the 200-West Area, including the U-8 and U-12 Cribs area, the water table is declining due to site-wide cessation of past (non-permitted) liquid effluent disposal practices. For example, between 1982 and 2002, the water levels dropped approximately 9 m (29 ft) [9].

APPROACH

The geophysical survey consisted of three phases: Phase I employed magnetic gradiometry and electromagnetic induction to identify metallic objects and anthropogenic features that may cause electrical interference. Phase II established a series of east-west and north-south electrical resistivity profiles (lines) across and adjacent to the Crib, which measures roughly 45 x 60 m (150 x 200 ft). Phase III collected information from more closely spaced profiles that were located based on the results of the Phase II survey.

THEORY

Much of the discussion presented in the “Theory,” “Methodology,” and “Results” sections are adopted from *HydroGeophysics 2010* [10].

Magnetic Gradiometry. Magnetic gradiometry attempts to quantify the earth’s magnetic field. The earth’s magnetic field is composed of three parts:

- Main Field – internal to the earth (i.e., emanating from a source within the earth, which slowly varies over time and space)
- Secondary Field – external to the earth, and varies rapidly in time
- Small Internal Fields – local magnetic anomalies in the near-surface crust, which are constant in time and space.

Magnetic anomalies are caused by magnetic minerals such as magnetite and pyrrhotite or buried metallic objects. The anomalies are measured by quantifying the contrast between magnetic susceptibility (k) versus background sediments. Sediments yield k values that average less than 1, compared to k values up to 20,000 for magnetic minerals.

A magnetic field results from either a point (dipole) source or a three-dimensional finite volume of magnetized material [11]. The magnetic field will decay in proportion to r^3 as the distance from the source increases, where r is the separation between the source and the magnetometer. The gradient of the magnetic field will decay in proportion to r^4 . A signal proportional to r^4 has more power at higher spatial frequencies compared to a signal proportional to r^3 (the field itself), by means of Fourier transform; therefore, the magnetic gradient signal generated from a three-dimensional source is more limited in spatial extent, causing discrete near-surface bodies to appear more pronounced compared to background readings.

Given a uniformly magnetized buried sphere, and when comparing both the total magnetic field and vertical magnetic gradient, both plotting methods are adequate for discriminating bodies in the near surface. However, the total field is only useful for determining deeply buried bodies.

The magnitude of the magnetic field or vertical magnetic gradient data is represented by isopleths on a contour map. Typically, the buried objects will appear as either a monopolar or a dipolar anomalous response. Infrastructure mapping of near-surface steel objects routinely yields magnetic field values several hundred to several thousand times higher than the background field. Linear anomalies recorded along adjacently acquired survey lines are interpreted as buried pipelines. In contrast, discontinuous singular anomalies are interpreted as discrete buried objects such as tanks, drums, wells, or metallic debris.

The magnetic field is measured with a magnetometer, of which there are two types—single- or dual-sensor. Single-sensor magnetometers measure the total magnetic field, and dual-sensor magnetometers (i.e., gradiometers) measure the gradient of the magnetic field.

Magnetometry is capable of providing useful information on the presence of buried metallic objects; however, a shortcoming of most magnetometers is that they record only total magnetic field and not separate components of a given vector field. This introduces uncertainty in the interpretation of the shape and intensity of a given anomaly, and can often portray the combined magnetic effects of several sources [12].

Electromagnetic Induction. Soils and bedrock have the ability to transmit electrical currents over tens or hundreds of meters depending on the material property of electrical conductivity. Soil and rock type, porosity, moisture content/degree of saturation, and dissolved salts/ionic constituents affect the relative effectiveness of electrical conductivity. Electromagnetic induction measures the electrical characteristics of various earth materials and is used to identify buried infrastructure within the area where resistivity data are collected.

Electromagnetic induction methods use a transmitting coil to induce eddy currents in the earth, which generate magnetic fields that are affected by the earth materials within this excited zone. A receiving coil intercepts the field, resulting in an output voltage that is proportional to the conductivity within the area. Buried features or objects can be identified by moving the transmitting and receiving coils and interpreting variations in conductivity. The depth of investigation for electromagnetic techniques is controlled by the transmitting coil frequency and the electrical conductivity of the host material, which in the case of the U-8 and U-12 Cribs are unconsolidated soils (sediments).

Electrical Resistivity. The resistivity method is based on the capacity of earth materials to resist electrical current, which (as with electrical conductivity) is a function of soil type, porosity, moisture, and dissolved salts. The concept behind applying the resistivity method is to detect and map changes in an imposed electrical field caused by heterogeneities in the subsurface. The resistivity method employs electric current (I) that is induced into the earth through one pair of metal rods, or electrodes (transmitting dipole) and measures the resultant voltage potential (V) across another pair of electrodes (receiving dipole). Field data are acquired using a multi-electrode array along linear transects; a multi-electrode array enables rapid data acquisition over a large area with minimal reconfiguration of equipment.

At U-Cribs, the progression of measurements occurred by moving one current electrode forward along the array and then measuring all adjacent voltage pairs inside the current pair. Once the roving current electrode reaches the end of a linear transect, the other current electrode at the beginning of the line moves forward incrementally while voltage is measured again (in ohm-meters) on all adjacent electrode pairs. Following acquisition, data are pre-processed to remove low-quality measurements (e.g., negative voltages, extremely high voltages, and data with high repeat errors), resulting from machine error, poor electrode placement, or poor electrode contact with surrounding sediment. Data quality is further assessed by contouring the pseudo-section comprised of the apparent resistivity at linear depth intervals associated with the separation distance between transmitting and receiving electrodes. This apparent

resistivity data are then processed through a nonlinear inverse model to obtain estimates of the true electrical resistivity of the subsurface that gave rise to the voltage measurements in the original data file.

METHODOLOGY

Survey Area and Logistics

The geophysical survey encompassed 37 acres (Fig. 1). Acquisition of data by magnetometer and electromagnetic induction (Phase I) was accomplished by employing an all-terrain vehicle that towed an equipment cart (geophysical operations cart or G.O. Cart). The G.O. Cart was towed along parallel lines spaced approximately 3 m apart. The G.O. Cart was equipped with two cesium-vapor magnetic sensors spaced 1 m apart vertically, a broadband electromagnetic sensor, a differential global positioning system (GPS) for geo-referencing of geophysical data, and a datalogger.

The Phase II electrical resistivity survey consisted of data collection along three lines with line lengths of 300 to 500 m. These widely spaced test lines were positioned to characterize the soil potentially impacted by the disposal activities at the Cribs, and to characterize background sediments.

The Phase III electrical resistivity survey consisted of data collection along 16 lines with line lengths of 250 m.

RESULTS AND INTERPRETATION

Phase I–Magnetic Gradiometry. The results from the magnetic gradiometry survey (both total magnetic field and vertical magnetic gradient) show several features that indicate known pipes, wells, or caissons. The caissons are buried concrete-lined vaults approximately 1 m in diameter, which received steam condensate from the U-Plant. Groundwater monitoring wells within the study area also showed a strong positive magnetic signature immediately south of the well locations.

Phase I–Electromagnetic Induction. The electromagnetic induction data represents in-phase (the real component of the data) and quadrature as electrical conductivity (the imaginary component of the data). The graphical representation of both the real and imaginary components is similar to the magnetic gradiometry results.

Phase II–Two Dimensional Electrical Resistivity. Fig. 4a (Test Line 2) and Fig. 4b (Test Lines 1 and 3) presents the results from the three test lines of Phase II, which consists of data that was inverted in two dimensions using RES2DINV.

RES2DINV. For Test Line 1, the inversion ran to five iterations for a final root mean square error of 1.09 percent, which is considered low and indicates excellent inversion model convergence. The resistivity data in Fig. 4b are presented in color contoured sections beside the plan map of their locations. Data are plotted as the logarithm of electrical resistivity to highlight low resistivity features that potentially are associated with past releases.

Test Line 1, located in part across the U-12 Crib (Fig. 4b), yielded a low-resistivity anomaly beneath the Crib. Other low-resistivity anomalies likely related to infrastructure or leaking pipes are indicated. For example, the pipeline at approximately 125 m along the line was detected (i.e., to the left of the crib), and another pipeline is indicated at 200 m along the line. The pipes at 50 and 75 m apparently were not detected by the electrical resistivity survey, but were detected by magnetometry.

Test Line 2, located in part across the U-8 Crib (Fig. 4a), yielded a near-surface low-resistivity anomaly directly below the Crib at a depth of 12 m, and again from 25 m to the water table (79 m [260 ft]). The geometry of this anomaly is consistent with the presumption that waste liquids reached groundwater.

Other than a pipe to the east of the Crib, metallic infrastructure does not appear to have affected the data at this location.

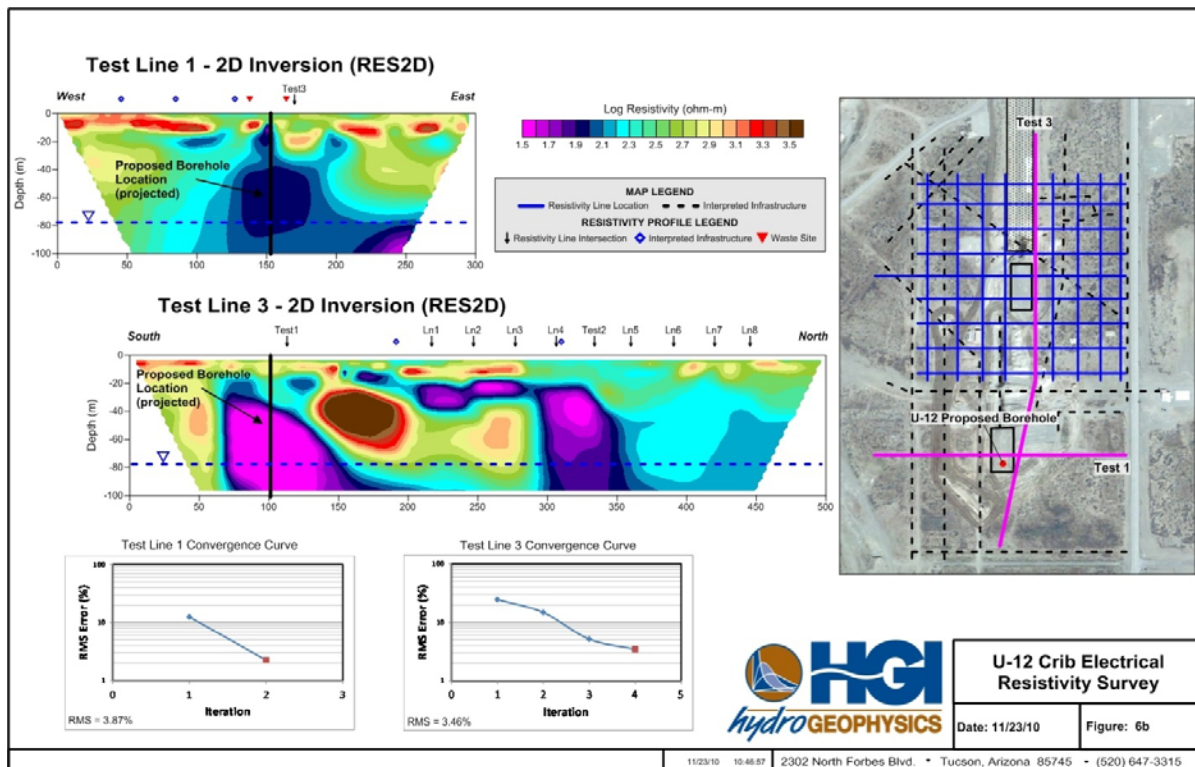
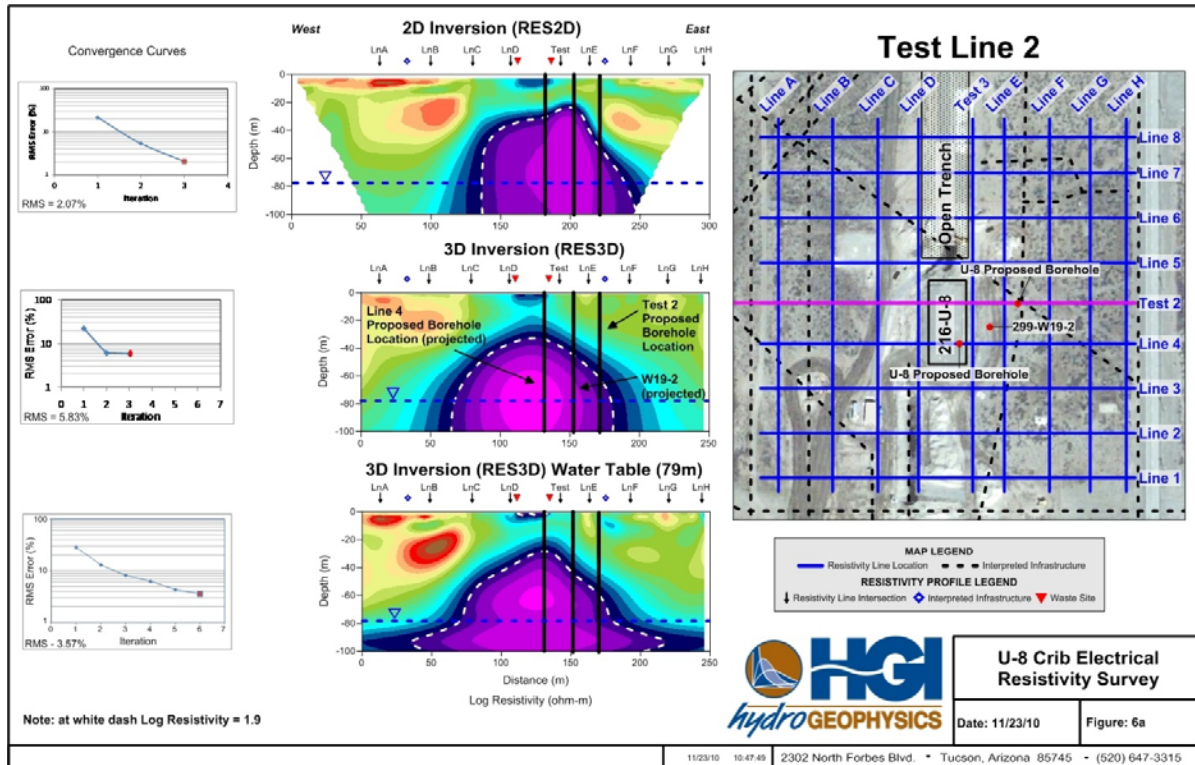


Fig. 4a. Comparison of two-dimensional and three-dimensional resistivity results across and adjacent to the U-8 Crib, showing the proposed borehole locations within and east of the Crib. Fig. 4b. Two-dimensional resistivity results across and adjacent to the U-12 Crib, showing the proposed borehole location within the Crib.

Test Line 3, the north-south line immediately east of both cribs (Fig. 4b), indicates the presence of low-resistivity features associated with both cribs. The apex of the low-resistivity cone at the U-12 Crib is located to the south of the Crib. The inferred contaminant concentration in this area is consistent with migration along the known southward dip of the Hanford formation sediments, before drainage to the water table. Due to three-dimensional effects in the acquisition and limitations of two-dimensional processing, the resistivity value of the anomaly is stronger in Test Line 3 than in Test Line 1.

At the U-8 Crib, the intensity of the north-south resistivity signal along Test Line 3 is similar to the intensity of the signal along Test Line 1; however, this two-dimensional processing yielded a discrepancy in the depth of the target, where the contours of the low-resistivity anomaly close above the water table in Test Line 3, unlike Test Line 1. The three-dimensional survey (discussed below) provides a measure of resolution to this discrepancy.

Phase III–Electrical Resistivity Across the U-8 Crib. The three-dimensional survey over the U-8 Crib consisted of 16 lines: data was collected along eight lines in an east-west direction and eight lines were run in a north-south direction. Prior to conducting three-dimensional inversion, the 16 additional survey lines were first processed by two-dimensional inversion using RES2DINV to perform a data quality analysis. This two-dimensional “final editing” step provided greater confidence in data quality.

The two-dimensional inversion results indicate a decrease in resistivity progressing toward the Crib.

RES3DINVx64 software was selected for three-dimensional inversion, utilizing 18 perpendicular lines and 57,530 data values. The inversion yielded a final root mean square error of 5.82 percent, and data were plotted in either Surfer or Rockworks software to visualize the subsurface. The results indicate a smooth, low-resistivity target directly beneath the U-8 Crib. The target apparently widens with depth in the deep vadose zone and increases in intensity as it approaches the water table.

Following the initial three-dimensional inversion modeling of the resistivity data, a series of models with a-priori information were completed to determine the influence of the water table on the model results. To address the apparent outward spreading of the low-resistivity target beneath the U-8 Crib, a-priori modeling of the water table was undertaken to better resolve the depth of low resistivity anomalies associated with the release by providing information about the water table (at 79 m) and its resistivity value. A-priori modeling solves for the best fitting solution within adjacent model layers that are based on actual field-measured data, such as the approximate location, dimensions and estimated resistivity of subsurface infrastructure, geologic layers, and hydrologic information such as the water table.

Four model test runs were completed to determine the most favorable a-priori values for resistivity and dampening factor for the water table. A value of 100 ohm-m was ultimately selected as the representative value for the water table, based on the improvement in resistivity distribution over no water table. Fig. 5 shows a volumetric rendering of the preferred three-dimensional inversion results, where image A shows a plan view (overhead) section, B shows an isometric view, C shows a cross section looking north, and D shows a cross section looking east.

Comparison of Electrical Resistivity Results to Soil Sampling Results. Nitrate data from historic boreholes at the U-8 and U-12 Cribs compared well with electricity resistivity anomalies and were used to calibrate resistivity data. Two-dimensional inversion data from Test Line 1 and Test Line 3 were compared to nitrate data (i.e., nitrogen in nitrate and nitrite) from borehole 299-W22-78, immediately east of the U-12 Crib (Fig. 6a).

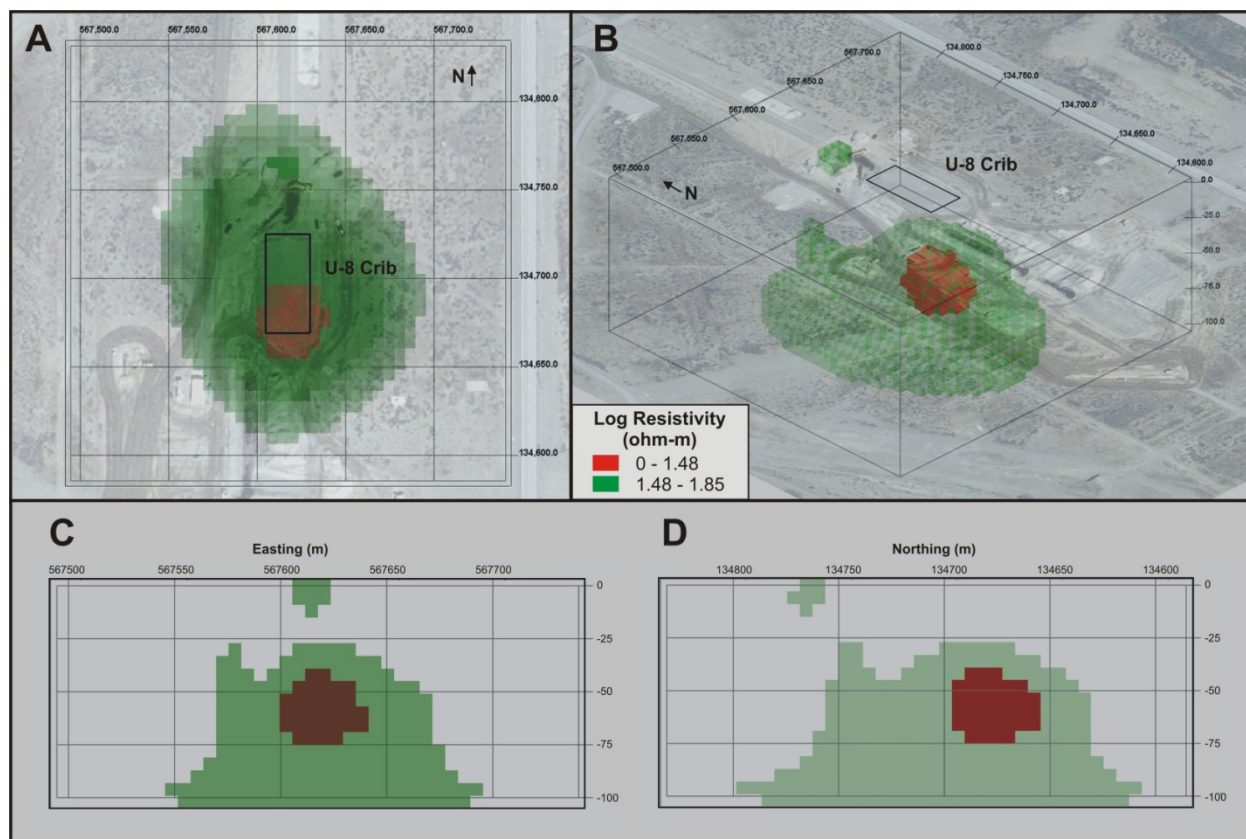


Fig. 5. Three-dimensional isometric view of three-dimensional inversion results, which includes the 100 ohm-m water table as an a-priori target.

Fig. 6a provides the profiles of nitrate concentration and resistivity from these lines (presented as electrical conductivity, the reciprocal of resistivity) and a scatterplot of co-located electrical conductivity and nitrate data. The upper 30 m of nitrate data correlated reasonably well with the electrical conductivity data. Correlation at depth may be compromised by water table effects (i.e., compare the low nitrogen concentration at 68 m to the electrical conductivity measurement in Test Line 3); this phenomena, and the discrepancy between Test Line 1 and Test Line 3, may be due to the limitations posed by two-dimensional treatment of a three-dimensional target. A full three-dimensional inversion model over the U-12 Crib would reconcile the target in both lines.

Fig. 6b provides the profiles of nitrate concentrations from borehole 299-W19-94 and electrical conductivity from the U-8 Crib. Correlation is indicated by the similar shapes of the two datasets. In general, a high in both nitrate and electrical conductivity is observed near the surface, reducing to lower values through the middle portion, before increasing again at depth.

In Fig. 6b, a discrepancy exists with the depth of the nitrate data, where the electrical conductivity data is closer to the surface by about 8 m. The relatively high electrical conductivity measurement at the 1 m depth may indicate a high nitrate soil concentration at that particular point along the geophysical survey line, thereby not reflecting the low nitrate concentration detected in the historic borehole; or, the electrical conductivity measurements at 1-5 m may represent an overcompensation effect from the influence of the high nitrate soil concentration measured at 10 m. Additionally, the intensity of the target at depth is much higher than the nitrate measured in soil at 28 m, 40 m, and 47 m, which may be caused by the water table. The employment of depth electrodes would enhance conductivity resolution deeper

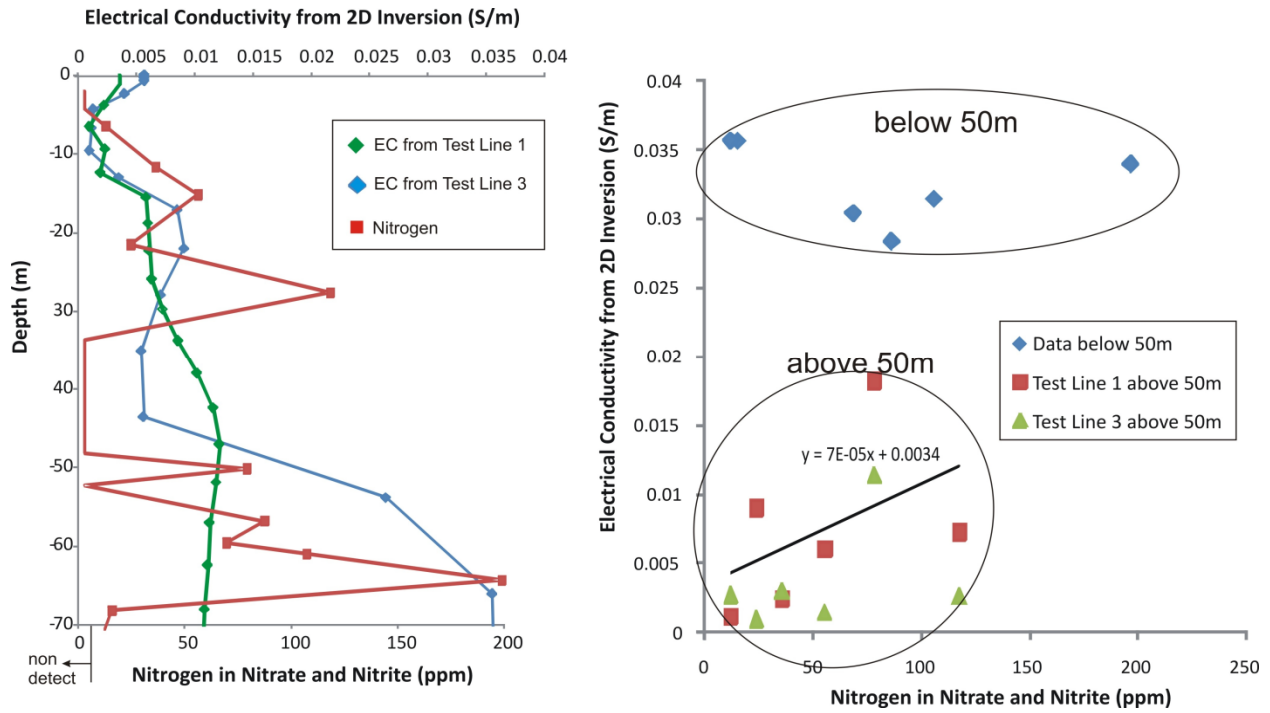
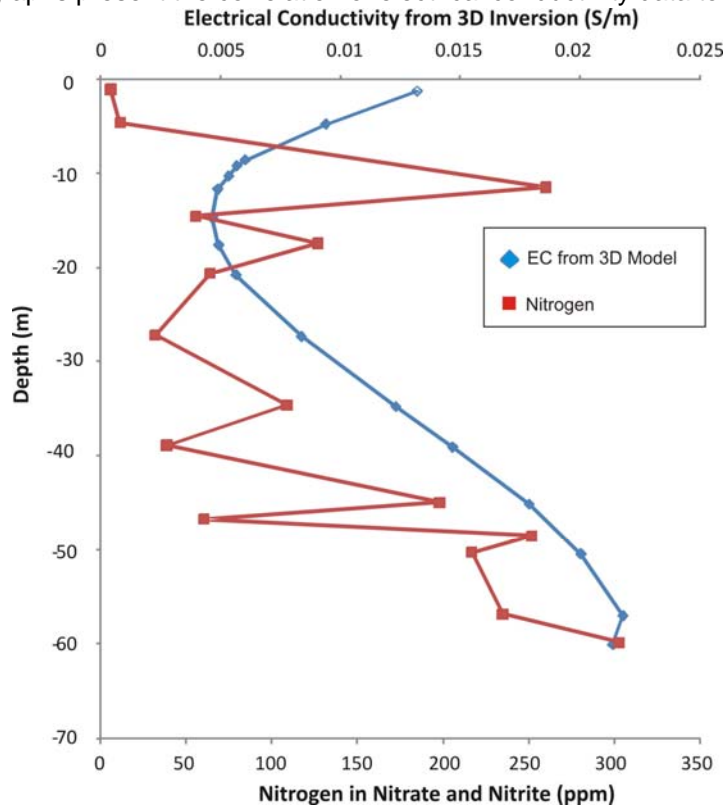


Fig. 6a. The upper graphs present the correlation of electrical conductivity data to nitrogen data from the



U-12 Crib. Fig. 6b. The lower graph presents the correlation of electrical conductivity data to nitrogen data from the U-8 Crib.

within the vadose zone. Better correlations could be obtained between conductivity and nitrate concentrations if additional sampling from deep characterization boreholes was completed.

BOREHOLE SELECTION BASED ON GEOPHYSICAL RESULTS

U-8 Crib Proposed Boreholes. Nitrate and radionuclide contamination has been confirmed within and adjacent to the U-8 Crib through historic drilling. Only one relatively deep borehole (299-W19-94, Fig. 2b and Fig. 6b) explored the vadose zone within or immediately adjacent to the Crib to a depth of 61 m (200 ft), which still leaves the deep vadose zone between 61-79 m (200-260 ft) without contaminant characterization. Therefore, additional characterization drilling is planned.

The results of both two-dimensional and three-dimensional inversion modeling from electrical resistivity data confirmed known contamination and provided information on the likely distribution of contamination beneath and adjacent to the U-8 Crib. Fig. 4a details two-dimensional and three-dimensional data along Test Line 2; provides the planned borehole locations for within the Crib and to the east of the Crib; and illustrates the predicted contaminant distribution that will be encountered when these boreholes are completed in 2011. Also shown is abandoned well 299-W19-2, which was completed to a depth of approximately 91 m (300 ft) in 1957. Contaminant information was not collected; however, at the time of well completion, the groundwater temperature in this well was recorded at 48°C (118°F), indicating that the process water being disposed of in the Crib was migrating to this well, which is located in a hydraulically downgradient position. The borehole planned near abandoned well 299-W19-2 will attempt to define the lateral extent of contamination, particularly at depths below 50 m (164 ft).

U-12 Crib Proposed Borehole. Nitrate and radionuclide contamination has been confirmed immediately adjacent to the U-12 Crib by one borehole (299-W22-78, Fig. 3a and Fig. 6a) through most of the vertical extent of the vadose zone, to a depth of 71 m (233 ft). Therefore, additional characterization drilling is planned for completion within the footprint of the U-12 Crib, to be advanced to the full vertical extent of the vadose zone. Fig. 4b presents the results of two-dimensional inversion modeling from electrical resistivity data, which illustrates the inferred contaminant distribution beneath and immediately adjacent to the crib. The actual contamination detected in borehole 299-W22-75 (within the U-12 Crib) and in borehole 299-W22-78 correlates well with the resistivity data collected across the crib; Fig. 3b provides a conceptualized view of contaminant distribution as indicated from this borehole data.

CONCLUSIONS

Magnetic gradiometry and electromagnetic induction were successful in identifying piping and other infrastructure in the vicinity of the U-8 and U-12 Crib. The identification of anthropogenic materials was important because their presence could have potentially been detrimental to the electrical resistivity survey. In particular, the mapping of pipelines helped refine the positions of the electrical resistivity survey lines.

Electrical resistivity data from three lines were inverted in two dimensions and showed that the method was viable to map subsurface conductivity despite interference from pipelines. Results of the test lines showed low-resistivity targets that appeared to correlate to the position of the U-8 and U-12 Crib and the high disposal volumes introduced to the subsurface.

Resistivity data from 18 perpendicular lines were inverted in three dimensions across the U-8 Crib, and further refined the apparent geometry of the highly conductive contaminant material throughout the vadose zone to the water table. A discrepancy exists between soil nitrate concentrations and electrical conductivity data from 1-5 m, and as the water table is approached (40-47 m). For the shallow discrepancy, it is possible that the placement of the geophysical survey line may not be detecting nitrate concentrations similar to those detected in the historic borehole. For both the shallow and deep

discrepancy, the geophysical results may represent an overcompensation effect from higher nitrate concentrations in soil below 0-10 m, and higher nitrate concentrations in groundwater at 79 m.

Overall, radionuclide and (in particular) nitrate contaminant distribution data from historic boreholes at the U-8 and U-12 Cribs compared well with electricity resistivity anomalies and were used to calibrate resistivity data; therefore, electrical resistivity mapping can be used to more accurately locate characterization boreholes.

REFERENCES

1. 40 CFR 300, “National Oil and Hazardous Substances Pollution Contingency Plan,” Appendix B, “National Priorities List,” *Code of Federal Regulations*.
2. CERCLA, *Comprehensive Environmental Response, Compensation, and Liability Act of 1980*, 42 USC 9601, et seq.
3. ECOLOGY, EPA, AND DOE, *Hanford Federal Facility Agreement and Consent Order*, 2 vols., as amended, Washington State Department of Ecology, U.S. Environmental Protection Agency, and U.S. Department of Energy, Olympia, Washington (1989).
4. *Hanford Soil Inventory Model*, RPP-26744, Rev. 1 (1994).
5. K.A. LINDSEY, *Miocene- to Pliocene-Aged Suprabasalt Sediments of the Hanford Site, South-Central Washington*, BHI-00184, Rev. 0, Bechtel Hanford, Inc., Richland, Washington (1995).
6. U.S. DEPARTMENT OF ENERGY (DOE). *Consultation Draft, Site Characterization Plan, Reference Repository Location, Hanford Site, Washington*, DOE/RW-0164, Vols. 1 and 2, U.S. Department of Energy, Office of Civilian Radioactive Waste Management, Washington, D.C. (1988).
7. K.A. LINDSEY, J.L. SLATE, G.K. JAEGER, K.J. SWETT, and R.B. MERCER, *Geologic Setting of the Low-Level Burial Grounds*, WHC-SD-EN-TI-290, Rev. 0, Westinghouse Hanford Company, Richland, Washington (1994).
8. B.A. WILLIAMS and C.J. CHOU, *Monitoring Plan for RCRA Groundwater Assessment at the 216-U-12 Crib L*, PNNL-14301, Pacific Northwest National Laboratory, Richland, Washington (2002).
9. B.A. WILLIAMS, B.N. BJORNSTAD, R. SCHALLA, and W.D. WEBBER, *Revised Hydrogeology for the Suprabasalt Aquifer System, 200-West Area and Vicinity, Hanford Site, Washington*, PNNL-13858, Pacific Northwest National Laboratory, Richland, Washington (2003).
10. HYDROGEOPHYSICS, INC., *Geophysical Characterization Of 216-U-8 And 216-U-12 Cribs Hanford, Washington*. RPT-2010-013, Rev. 1 (2010).
11. F.S. GRANT and G.F. WEST, *Interpretation Theory in Applied Geophysics*, McGraw Hill Co., New York (1965).
12. S. BREINER, *Applications Manual for Portable Magnetometers*, Geometrics, Inc. San Jose, California (1973).